The leading edge effect in a suddenly differentially heated cavity

F. Xu[1] J. C. Patterson[2] C. Lei[3]

(Received 31 August 2006; revised 19 December 2007)

Abstract

We perform a two dimensional numerical simulation of transient natural convection in a suddenly differentially heated cavity in order to observe the initial transient flows, particularly the leading edge effect. The numerical results show that the pressure plays a key role in the origination and propagation of the leading edge effect and the deviation of the numerical solution from the theoretical solution is due to the neglect of the convection terms in the theoretical solution of the energy equation. Accordingly, the one dimensional conduction solution does not estimate the transport coefficients.

Contents

See http://anziamj.austms.org.au/ojs/index.php/ANZIAMJ/article/view/134 for this article, Published December 31, 2007. ISSN 1446-8735

1 Introduction

For a suddenly heated vertical surface, which could be either a flat plate or a sidewall of a differentially heated cavity, Goldstein and Briggs [4] indicated that the early transient response is one dimensional and the heat transfer from the surface to the fluid is dominated by conduction. Before the vertical thermal boundary layer flow approaches a steady state, an overshoot of its temperature followed by a few disturbances, is firstly achieved. The overshoot and disturbances comprise the leading edge effect (LEE), which originates from the leading edge of the sidewall or semi-infinite flat plate, and propagates downstream [3, 6]. The LEE is one of the noticeable features in the initial development of the thermal boundary layer flow for the case of sudden heating. An important aspect of describing the LEE propagation is to predict its arrival time at any downstream location, and an analytical solution of the one dimensional thermal boundary layer equation [4] was often employed to calculate the arrival time. However, Mahajan and Gebhart [5] demonstrated that the prediction based on the analytical solution [4] significantly lagged behind the experimental measurements. Armfield and Patterson [1] indicated that the speed of the unstable traveling waves in the thermal boundary layer, based on a linear stability analysis, is consistent with

that of the LEE propagation, which is also supported by experiments [6]. This implies that the waves in the LEE region are a result of the thermal boundary layer instability. Armfield and Patterson [2] based on numerical simulations suggested that the LEE propagation could be based on two speeds, a faster speed and a slower speed. Evidently, this speculation of the LEE propagation based on two speeds needs further validation.

In this article, a two dimensional numerical simulation of natural convection in a suddenly differentially heated cavity is performed and major physical variables such as pressure, temperature and velocities in the vicinity of the sidewall of the cavity are examined. The dynamic mechanisms of the origination and propagation of the LEE are discussed. We find that the LEE is indeed an interaction coupling temperature, pressure and velocities, and the pressure perturbations plays a key role in the origination and propagation of the LEE.

2 Numerical procedures

The two dimensional Navier–Stokes and energy equations with the Boussinesq approximation to be solved are

$$\frac{\partial u}{\partial x}+\frac{\partial v}{\partial y}=0\,, \tag{1}$$

$$\frac{\partial u}{\partial t}+u\frac{\partial u}{\partial x}+v\frac{\partial u}{\partial y}=-\frac{1}{\rho}\frac{\partial p}{\partial x}+\nu\left(\frac{\partial^2 u}{\partial x^2}+\frac{\partial^2 u}{\partial y^2}\right)\,, \tag{2}$$

$$\frac{\partial v}{\partial t}+u\frac{\partial v}{\partial x}+v\frac{\partial v}{\partial y}=-\frac{1}{\rho}\frac{\partial p}{\partial y}+\nu\left(\frac{\partial^2 v}{\partial x^2}+\frac{\partial^2 v}{\partial y^2}\right)+g\beta(T-T_0)\,, \tag{3}$$

$$\frac{\partial T}{\partial t}+u\frac{\partial T}{\partial x}+v\frac{\partial T}{\partial y}=\kappa\left(\frac{\partial^2 T}{\partial x^2}+\frac{\partial^2 T}{\partial y^2}\right)\,, \tag{4}$$

where T is the temperature, T_0 is the initial mean temperature, p is the pressure, u is the velocity in the x-direction, v is the velocity in the y-direction,

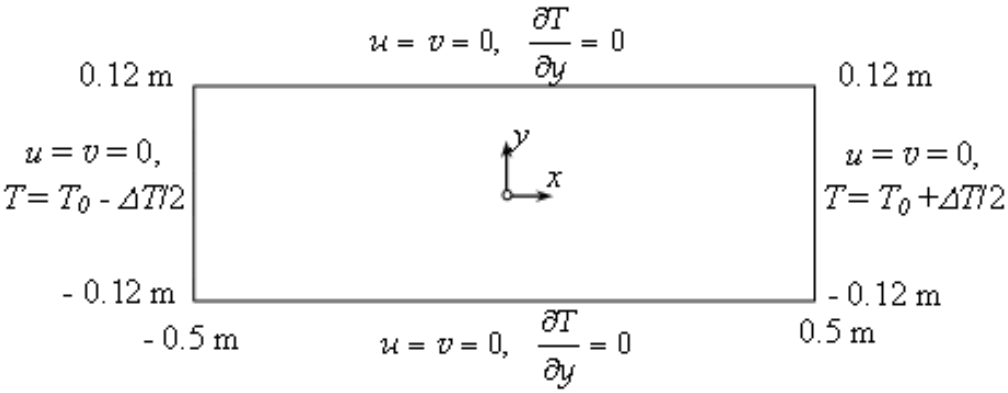

FIGURE 1: Schematic of the computational domain and boundary conditions.

g is the acceleration due to gravity, ρ is the density, β is the coefficient of thermal expansion, κ is the thermal diffusivity, and ν is the kinematic viscosity. SI units are adopted for all quantities throughout the article.

A two dimensional domain (see Figure 1), which is $H = 0.24\,\mathrm{m}$ high by $L = 1\,\mathrm{m}$ long, is considered based on an experimental model [9]. The working fluid is water, which is isothermal ($T_0 = 295.55\,\mathrm{K}$) and motionless at the initial time. All boundary conditions are shown in Figure 1 with a temperature difference of 16 K between two sidewalls. The corresponding Rayleigh and Prandtl numbers are 3.77×10^9 and 6.64, respectively:

$$\mathrm{Ra} = \frac{g\beta\Delta T H^3}{\nu\kappa} \quad \text{and} \quad \mathrm{Pr} = \frac{\nu}{\kappa}. \tag{5}$$

The governing equations are solved using the SIMPLE scheme. The spatial derivatives are discretized with a second-order upwind scheme for the advection terms, and time marching is performed by a second order implicit scheme.

Two non-uniform grids (199×563 and 395×1155) with an expansion

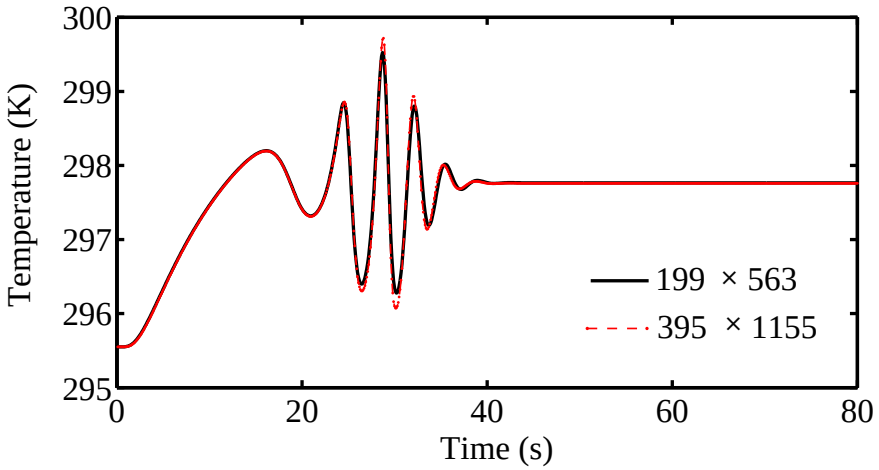

FIGURE 2: Temperature series calculated by using different grids at point (0.498 m, 0.09 m).

factor from the wall surface to the interior are tested. The unsteady results calculated using the different grids are shown in Figure 2, which plots the time series of the temperatures at the point (0.498 m, 0.09 m) within the boundary layer in the early stage. Clearly, the two time series of the temperatures calculated using the two grids vary slightly during the period when unstable waves are present (corresponding to the period with distinct peaks and troughs on the plots). At other times, these two plots overlap with each other. Therefore, to reduce computing time, the grid 199×563 is adopted in our calculations.

A time step of 0.1 s is adopted based on previous numerical simulation [8] in which it has been demonstrated that this time step is sufficient to capture the features of the transient flows, and the stability of the scheme is also guaranteed with the adoption of the non-uniform grids.

3 Origin of the leading edge effect

In a differentially heated cavity, the leading edge of the thermal boundary layer is the join of the isothermal vertical sidewall and the adiabatic horizontal bottom wall at the upstream corner. In order to obtain some insights into the dynamic mechanisms responsible for the generation and propagation of the LEE, the discussion here starts from the origin of the LEE, that is, the upstream corner. Figure 3 shows the pressure, velocity and temperature fields near the upstream corner of the thermal boundary layer in the initial stage. Although the times are very small (1 s and 3 s), the flow near the corner is two dimensional. This is a result of the mass transfer in the corner region; that is, following the sudden heating, the heated fluid in the upstream corner is convected upwards due to the buoyancy effect, and in the meantime the fluid outside the upstream corner, which is colder than that in the upstream corner, is entrained into the corner, as seen in Figure 3. Figure 3(a) indicates that the pressure minimum firstly arises in the upstream corner in the initial stage, resulting in a negative pressure gradient toward the corner. Figure 3(b) shows that the low pressure zone near the corner extends outwards and the entrainment into the corner becomes increasingly stronger (indicated by the relative length of the velocity vectors). The temperature contours at different times in Figures 3(a) and (b) indicate that the thickness of the vertical thermal boundary layer grows with time. Since the temperature of the fluid entrained into the upstream corner is lower than that of the heated fluid in the upstream corner and the viscous effect of the velocity field due to the adiabatic bottom boundary is present, a temperature contour ($T = 295.56\,\mathrm{K}$), convex to the hot sidewall, results as seen in Figure 3(b).

In summary, the sudden heating of the sidewall results in a temperature variation (distribution) of the fluid in the vicinity of the sidewall by conduction in the initial stage, which in turn produces a buoyancy force driving the heated fluid upwards adjacent to the sidewall. When the heated fluid near the leading edge moves upwards, the mass balance (through the continuity equation (1)) induces a pressure distribution (that is, a pressure minimum

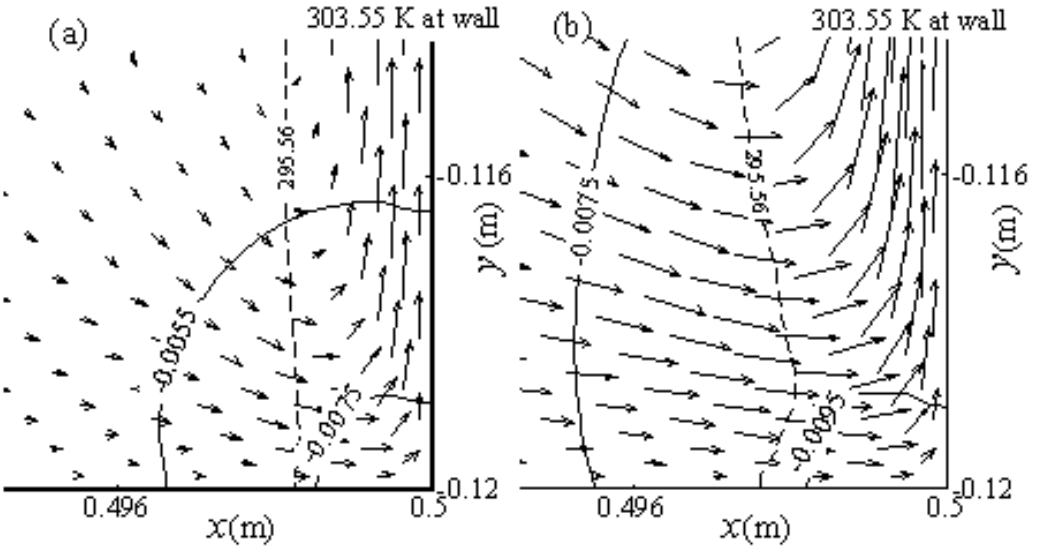

FIGURE 3: Isotherms (dashed line), isobars (solid line), and velocity vectors near the bottom corner at two early times. (a) $t = 1\,\mathrm{s}$. (b) $t = 3\,\mathrm{s}$.

arises near the leading edge) which drives the horizontal entrainment near the leading edge (see Figures 3 and 4). As a consequence, the pressure gradient, as the only horizontal force, plays a key role in the origination of the LEE.

4 Propagation of the leading edge effect

For the purpose of illustrating the propagation of the pressure perturbations, Figure 4 shows the pressure contours and the corresponding streamlines at different times. As the pressure minimum moves downstream, by comparing stream function values at different times, Figure 4 shows that the convection at the upstream side of the pressure minimum is apparently enforced. In particular, the horizontal convection in which the pressure gradient is the only driving force significantly increases with time. Figure 4(f) also shows the vectors of the negative pressure gradient at $t = 6.2\,\mathrm{s}$. Clearly, the horizontal entrainment is driven by the pressure gradient near the location of the pressure minimum.

In order to observe further the temperature variation associated with the propagation of the LEE, Figure 5 plots time series of the temperatures at different heights. Distinct properties of the LEE propagation, such as the overshoot of the temperatures and the increasing amplitude of the traveling waves with height following the overshoot, are shown. The times when the temperature achieves the first peak at different heights in Figure 5 correspond to those in Figure 4 in which the pressure contours and stream functions are shown. By comparing the location of the temperature peak (see the height of each curve in Figure 5) with that of the pressure minimum (see the pressure contour within the contour of $-0.0035\,\mathrm{Pa}$) at the same time, we find that the former location is higher than the latter one; that is, the temperature maximum first arises at certain point in the thermal boundary layer, and then the pressure minimum arrives. Furthermore, the numerically calculated

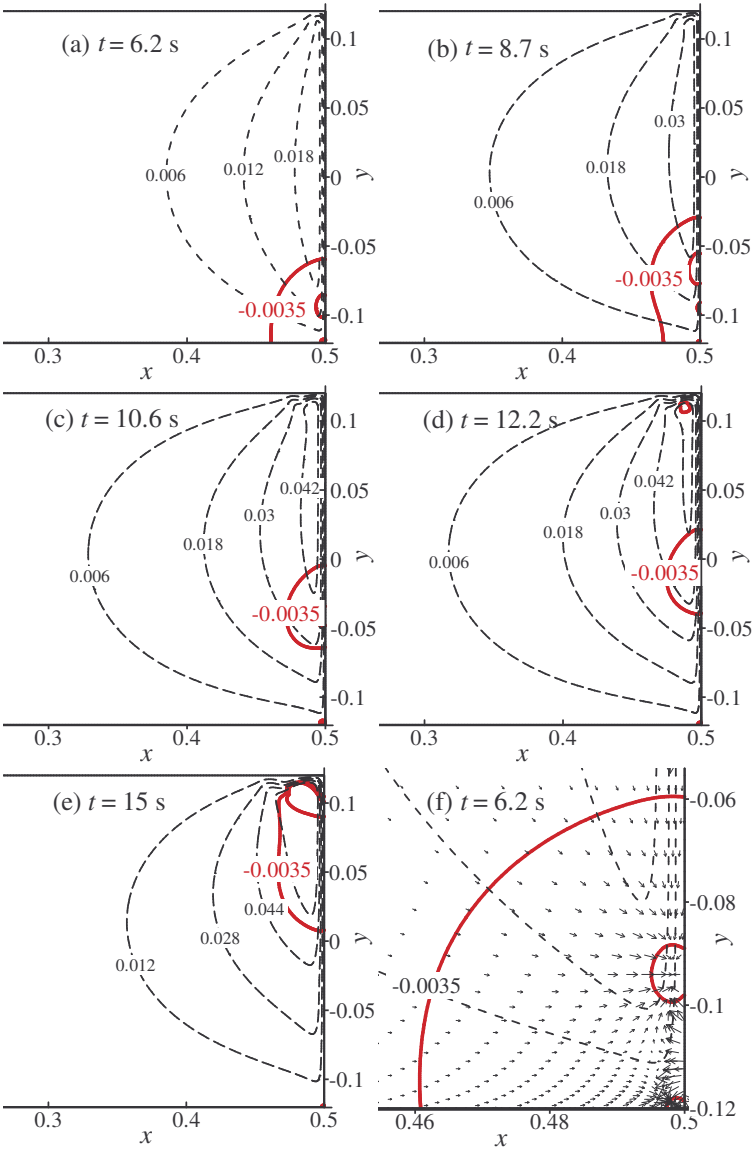

FIGURE 4: Isobars (solid lines) and streamlines (dashed lines) adjacent to the hot sidewall (vectors in (f): negative pressure gradients).

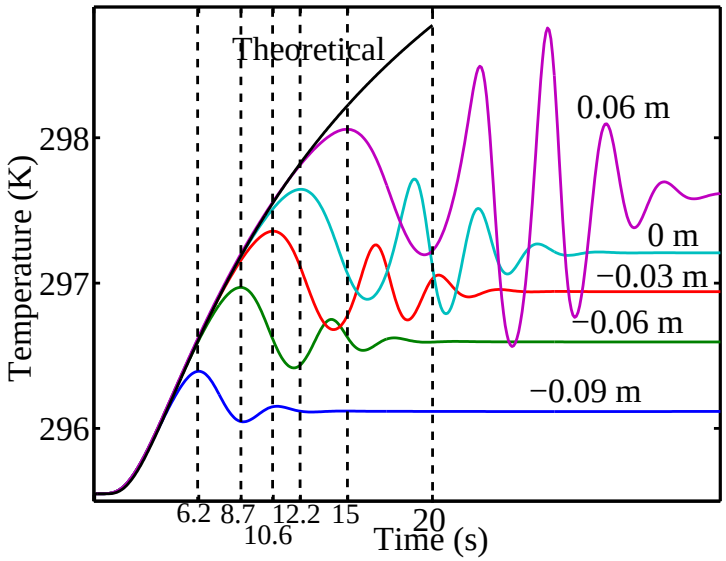

FIGURE 5: Time series of the temperatures at different heights ($x = 0.498$ m).

temperature apparently deviates from the theoretical solution [4], as seen in Figure 5.

For the purpose of measuring the speed of the LEE, Figure 6 plots the locations of the pressure minimum, the temperature maximum and the deviation of the numerical solution from the theoretical solution measured from the bottom against the time squared. Clearly, there is a very good linear correlation between the locations and the time squared for the three sets of data in the initial stage; that is, the propagation speeds of the pressure minimum, the temperature maximum and the deviation of the numerical solution from the theoretical solution are a linear function of time, which is also coincidently consistent with the scaling prediction of the initial flow velocity (that is, $v \sim t$) by Patterson and Imberger [7].

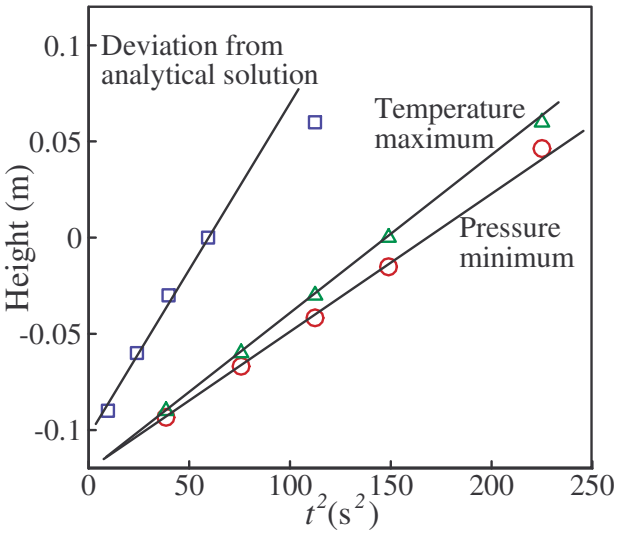

FIGURE 6: Locations of the pressure minimum, the temperature maximum and the deviation of the numerical solution from the theoretical solution measured from the bottom against t^2.

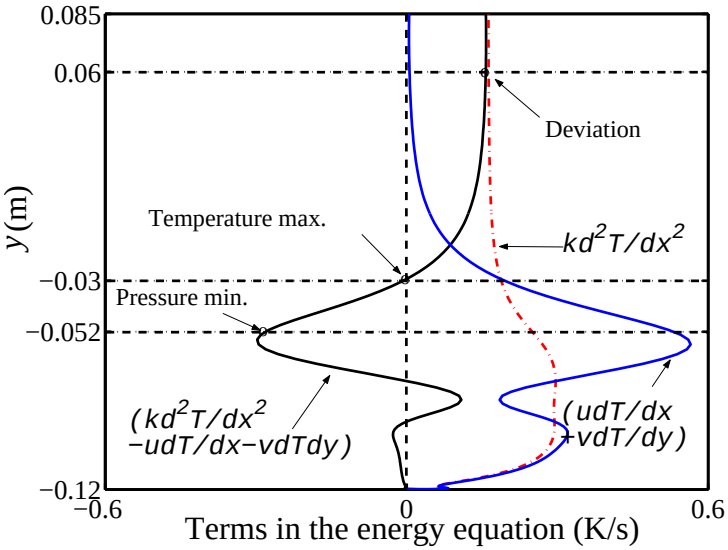

FIGURE 7: Terms in the energy equation at $x = 0.498\,\mathrm{m}$ at $t = 10.6\,\mathrm{s}$.

5 Heat balance in the initial stage

In order to obtain insights into the deviation of the numerical solution from the theoretical solution [4], the components of the energy equation (4) are discussed in this section. Both the numerical and theoretical solutions of temperature are obtained by solving the energy equation.

Figure 7 shows the vertical profile of each term in the energy equation at $t = 10.6\,\mathrm{s}$. The diffusion term ($k\partial^2T/\partial x^2$) is approximately constant far downstream of the pressure minimum and significantly increases upstream of the pressure minimum point. Similarly, the convection terms ($u\partial T/\partial x + v\partial T/\partial y$) are approximately zero downstream of the deviation point ($y = 0.06\,\mathrm{m}$, see Figure 7). However, upstream of $y = 0.06\,\mathrm{m}$, the convection terms increase as the distance from the deviation point increases. As a consequence, the unsteady temperature term ($k\partial^2T/\partial x^2 - u\partial T/\partial x -$

$v\partial T/\partial y$) also deviates away from the approximate coincidence with the diffusion term. This observation indicates the reason why the numerical solution apparently deviates from the theoretical solution (also see Figures 5 and 6); that is, the deviation is a result of the neglect of the convection terms in the theoretical solution of the energy equation [4].

As the convection term increases and eventually balances the diffusion term at $y = -0.03\,\mathrm{m}$, the unsteady temperature term is equal to zero at this point (Figure 7) and the temperature reaches the maximum (refer Figure 6). The pressure minimum point is in the upstream of the temperature maximum and does not coincide with the maximum of the convection terms as seen in Figure 7. Upstream of the pressure minimum, perturbations of the LEE are clear. Armfield and Patterson [2] indicated that the propagation speed of the LEE perturbations is determined by the speed of traveling waves based on the stability analysis.

6 Conclusions

As indicated in Figures 3 to 5, the LEE is an interaction among the major flow quantities including the temperature, pressure and velocities. In particular, the pressure (that is, the pressure gradient) plays a key role in the origination and propagation of the LEE. A good linear correlation of the locations of the pressure minimum, the temperature maximum and the deviation with the time squared illustrates that the different propagation speeds of these quantities describing the LEE linearly increase with time in the initial stage (Figure 6). Furthermore, the numerical solution significantly deviates from the theoretical solution due to the neglect of the convection terms in the theoretical solution.

Acknowledgement: The financial support of the Australian Research Council is gratefully acknowledged.

References

[1] Armfield, S. W. and Patterson, J. C., Wave properties of natural-convection boundary layers, *J. Fluid Mech.*, **239**, 195–211, 1992. doi:10.1017/S0022112092004373 C791

[2] Armfield, S. W. and Patterson, J. C., Start-up flow on a vertical semi-infinite heated plate, *Proc. 7th Australasian Heat and Mass Transfer*, Townsville, 37–43, 2000. C792, C802

[3] Gebhart, B., Transient response and disturbance growth in vertical buoyancy-driven flows, *J. Heat Transfer*, **110**, 1166–1174, 1988. C791

[4] Goldstein, R. J. and Briggs, D. G., Transient free convection about vertical plates and cylinders, *J. Heat Transfer*, **86**, 490–500, 1964. C791, C799, C801, C802

[5] Mahajan, R. L. and Gebhart, B., Leading edge effects in transient natural convection flow adjacent to a vertical surface, *J. Heat Transfer*, **100**, 731–733, 1978. C791

[6] Patterson, J. C., Graham, T., Schpf, W. and Armfield, S. W., Boundary layer development on a semi-infinite suddenly heated vertical plate, *J. Fluid Mech.*, **453**, 39–55, 2002. doi:10.1017/S0022112001006553 C791, C792

[7] Patterson, J. C. and Imberger, J., Unsteady natural convection in a rectangular cavity, *J. Fluid Mech.*, **100**, 65–86, 1980. doi:10.1017/S0022112080001012 C799

[8] Xu, F., Patterson, J. C. and Lei, C., Oscillations of the Horizontal Intrusion in a Side-heated Cavity, *15th Australasian Fluid Mechanics Conference*, Sydney, 779–782, 2004. C794

[9] Xu, F., Patterson, J. C. and Lei, C., Shadowgraph observations of the transition of the thermal boundary layer in a side-heated cavity, *Exp. Fluids*, **38**, 770–779, 2005. doi:10.1007/s00348-005-0960-1 C793

Author addresses

1. **F. Xu**, School of Engineering, James Cook University, Townsville, Australia.
mailto:feng.xu@jcu.edu.au

2. **J. C. Patterson**, School of Engineering, James Cook University, Townsville, Australia.

3. **C. Lei**, School of Engineering, James Cook University, Townsville, Australia.